A Structural Limitation on Enzyme Activity: The Case of HMG-CoA Synthase[†,‡]

Calvin N. Steussy,*[,§] Aaron D. Robison,[||] Alison M. Tetrick,[||] Jeffrey T. Knight,[||] Victor W. Rodwell,[⊥] Cynthia V. Stauffacher,[#] and Autumn L. Sutherlin[||]

Department of Biological Sciences, Department of Biochemistry, and Purdue Cancer Center, Purdue University, West Lafayette, Indiana 47907, and Department of Chemistry and Biochemistry, Abilene Christian University, Abilene, Texas 79699

Received July 26, 2006; Revised Manuscript Received September 29, 2006

ABSTRACT: Recent structural studies of the HMG-CoA synthase members of the thiolase superfamily have shown that the catalytic loop containing the nucleophilic cysteine follows the ϕ and ψ angle pattern of a II′ β turn. However, the $i + 1$ residue is conserved as an alanine, which is quite unusual in this position as it must adopt a strained positive ϕ angle to accommodate the geometry of the turn. To assess the effect of the conserved strain in the catalytic loop, alanine 110 of *Enterococcus faecalis* 3-hydroxy-3-methylglutaryl coenzyme A (HMG-CoA) synthase was mutated to a glycine. Subsequent enzymatic studies showed that the overall reaction rate of the enzyme was increased 140-fold. An X-ray crystallographic study of the Ala110Gly mutant enzyme demonstrated unanticipated adjustments in the active site that resulted in additional stabilization of all three steps of the reaction pathway. The rates of acetylation and hydrolysis of the mutant enzyme increased because the amide nitrogen of Ser308 shifts 0.4 Å toward the catalytic cysteine residue. This motion positions the nitrogen to better stabilize the intermediate negative charge that develops on the carbonyl oxygen of the acetyl group during both the formation of the acyl-enzyme intermediate and its hydrolysis. In addition, the hydroxyl of Ser308 rotates 120° to a position where it is able to stabilize the carbanion intermediate formed by the methyl group of the acetyl-S-enzyme during its condensation with acetoacetyl-CoA.

Two distinct metabolic pathways form isopentenyl diphosphate (IPP),[1] the precursor of isoprenoids in all forms of life. Eukaryotea and archaea produce IPP by the mevalonate pathway that converts three molecules of acetyl-CoA to IPP (*1*). In eukaryotic cells IPP is the basic building block for the synthesis of such biologically important molecules as steroid hormones, farnesyl pyrophosphate, and cholesterol, and mevalonate pathway enzymes have proven to be effective targets for cholesterol-lowering drugs. In contrast, most bacteria produce IPP by a pathway that converts pyruvate and glyceraldehyde 3-phosphate to IPP (*2*) where it is used in the production of undecaprenol which is involved in cell wall biosynthesis (*3*), menaquinones and ubiquinones which function in electron transport (*4*), and the light-harvesting carotenoids (*5*). However, a number of pathogenic, Gram-positive bacteria such as *Enterococcus faecalis*, *Staphylococcus aureus*, and *Streptococcus pneumoniae* utilize a mevalonate pathway parallel to that found in eukaryotes (*6*). This pathway has been shown to be essential for their survival, as knockout mutants of HMG-CoA synthase, the second enzyme in the pathway, in both *S. aureus* and *S. pneumoniae* require externally provided mevalonate to survive (*7*). This raises the possibility of developing a small molecule inhibitor to the prokaryotic HMGS that would serve as a highly specific antimicrobial agent.

Targeting the mevalonate pathway for an antibiotic might appear to be problematic as mevalonate is utilized for IPP synthesis in the host as well as the pathogens. However, the eukaryotic and prokaryotic synthetic enzymes differ in significant ways. For example, distinct prokaryotic and eukaryotic classes of HMG-CoA reductase, the third enzyme of the mevalonate pathway, have been identified on the basis of sequence, structure, and response to inhibitors (*8*−*10*). On the basis of sequence comparison, HMG-CoA synthase appears to have at least three distinguishable forms: cytosolic, mitochondrial, and bacterial (*11*). These isoforms all have different major end products such as cholesterol for

[†] This work was supported by a grant from the National Institutes of Health, Heart, Lung and Blood Institute (HL 52115), and from the National Science Foundation (MCB 0444247), both awarded to C.V.S. Support for A.L.S. came from a grant from The Welch Foundation (R-0021). A.L.S. also acknowledges the financial and intellectual support of the ACU Math-Science Research Council for undergraduate student research in her department. Support of the core facilities for macromolecular crystallography is provided in part through a grant to the Purdue Cancer Center from the National Cancer Institute (NCI CA23168) and by the Markey Center for Structural Biology, Purdue University. Use of the Advanced Photon Source was supported by the U.S. Department of Energy, Basic Energy Sciences, Office of Science, under Contract W-31-109-Eng-38. Use of the BioCARS Sector 14 was supported by the National Institutes of Health, National Center for Research Resources (RR07707).

[‡] The coordinates and structure factors for HMG-CoA synthase mutant enzyme Ala110Gly presented herein have been deposited in the Protein Data Bank and can be accessed with the code number 2HDB.

* Corresponding author: e-mail, csteussy@purdue.edu; tel, 765-496-3131; fax, 765-496-1189.

[§] Department of Biological Sciences, Purdue University.

[||] Department of Chemistry and Biochemistry, Abilene Christian University.

[⊥] Department of Biochemistry, Purdue University.

[#] Department of Biological Sciences and Purdue Cancer Center, Purdue University.

[1] Abbreviations: HMG-CoA, 3-hydroxy-3-methylglutaryl coenzyme A; HMGS, HMG-CoA synthase; IPP, isopentenyl diphosphate; IPTG, isopropyl β-D-thiogalactopyranoside; CoA, coenzyme A.

10.1021/bi061505q CCC: $33.50
Published on Web 11/09/2006

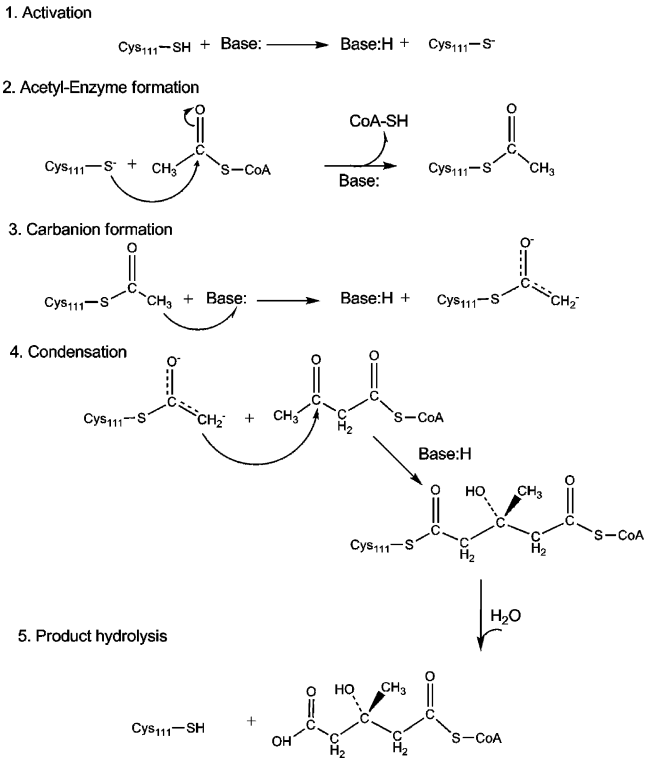

FIGURE 1: Mechanism of HMG-CoA synthase. For this general mechanism the active site cysteine is labeled as Cys111.

the eukaryotic−cytoplasmic, ketone bodies for the mitochondrial, and undecaprenol for bacterial HMGS. The differences between the prokaryotic and eukaryotic enzymes of this pathway suggest that inhibitors specific for the bacterial enzymes could be developed as antibiotics for these Gram-positive pathogens.

HMGS catalyzes the second reaction in the isoprenoid pathway, the irreversible condensation of acetoacetyl-CoA and acetyl-CoA to form HMG-CoA, by a multistep mechanism (Figure 1) (*12*−*14*). In the first step, the active site cysteine is activated by a base to serve as a nucleophile. This activated cysteine then attacks the carbonyl carbon of the thioester acetyl-CoA, the first substrate. Subsequent transfer of the acetyl group from the coenzyme A to the Sγ of the cysteine creates an acetyl-enzyme thioester and releases the reduced coenzyme A (Figure 1, steps 1 and 2). In the subsequent condensation step the methyl group of the acetyl-enzyme complex is promoted to a carbanion by an interaction with another base, thought to be Glu79 in *E. faecalis* HMGS (Figure 1, step 3) (*15*, *16*). The nucleophilic carbanion attacks the distal (γ) carbonyl of the second substrate, acetoacetyl-CoA, leading to the formation of a CoA-HMG-enzyme intermediate (Figure 1, step 4). The final step is the hydrolysis of the HMG-enzyme thioester that releases HMG-CoA and regenerates the reduced cysteine of the enzyme (Figure 1, step 5).

Recently published structures of HMGS enzymes from the pathogens *E. faecalis* (*17*) and *S. aureus* (*16*, *18*) demonstrate that these enzymes share the classic thiolase fold (*19*) with other condensing enzymes such as bacterial and human thiolase (*20*), chalcone synthase from alfalfa (*21*), and β-ketoacyl ACP synthases I (*22*), II (*19*), and III (*23*) from *Escherichia coli*. This motif likely arose from a gene duplication event that resulted in mirrored secondary structure topologies of the N- and C-terminal subdomains of the monomer (Figure 2). The secondary structure sequence for each subdomain is a β-α-β-α-β-α-β-β sequence. The two duplicated halves fold into a monomer structure with two central helices surrounded by β sheets with a final layer of α helices on the outside. The monomers associate as a dimer, thought to be the biologically active unit, with their β strands aligned to create a 10-strand β structure that traverses the molecule (Figure 3).

The active site cysteine of HMGS, residue 111, is on a loop in the N-terminal subdomain between β strand Nβ3 and the innermost α helix, Nα3 (Figure 2, indicated in green). This loop has the same series of ϕ and ψ angles as a type II′ β turn. However, the published HMGS structures show that the $i + 1$ residue located immediately N-terminal to the catalytic cysteine is an alanine. This is unusual in that the residue in this position of the turn is forced to have a positive ϕ angle in order to accommodate the geometry of the bend. A non-glycine residue with this ϕ angle has a steric clash between the Cβ hydrogens and the preceding carbonyl oxygen that has been shown experimentally to require 1.2 kcal/mol of energy to maintain (*24*). It is not surprising then that the $i + 1$ position of a II′ β turn was found to be overwhelmingly a glycine in a recent survey of β turns from high-resolution protein structures (*25*). This raises the question why this residue has not been mutated by nature to a glycine that would leave the enzyme in a lower, and presumably more stable, energy state. However, a review of the sequence alignments of HMGS enzymes from humans to plants to bacteria, which presumably share the same active site configuration, shows that this strained alanine residue has been selectively conserved (*17*). Review of the published structures of the broader group of thiolases demonstrates that they also have catalytic loops with II′ β turn geometries. In these catalytic turns a sterically clashing $i + 1$ residue is conserved in the human biosynthetic cytosolic (PDB code 1WL4) and mitochondrial (PDB code 2F2S) thiolases, bacterial thiolases (PDB code 1DM3), and bacterial β-ketoacyl ACP synthases (PDB codes 1FJ8, 1ALM, 1EBL). The exception is the condensing enzyme chalcone synthase from alfalfa that has a nonclashing glycine in the $i + 1$ position, demonstrating that in some circumstances the hidden hand of natural selection does choose a lower energy state for the catalytic loop. The persistence of this sterically clashing residue and the resulting strained catalytic loop of this enzyme family piqued our interest, and so a mutation at this position from alanine to glycine was made in HMG-CoA synthase from *E. faecalis* to evaluate its effect on the kinetics of the enzyme and the structure of the active site.

MATERIALS AND METHODS

Reagents. Purchased reagents and kits included 40% acrylamide, Bradford reagent, and MicroSpin BioP-30 columns (Bio-Rad), isopropyl β-D-thiogalactopyranoside (IPTG) (Gold Biotechnology, Inc.), Talon purification kit (Clontech Laboratories, Inc.), QuikChange site-directed mutagenesis kit and StrataPrep plasmid miniprep kit (Stratagene). Synthetic oligonucleotides were prepared by Integrated DNA Technologies (Coralville, IA). Unless otherwise specified, all other reagents were from Sigma.

Construction of the Mutant Plasmid. The alanine 110 to glycine mutation was introduced into the *E. faecalis mvaS*-

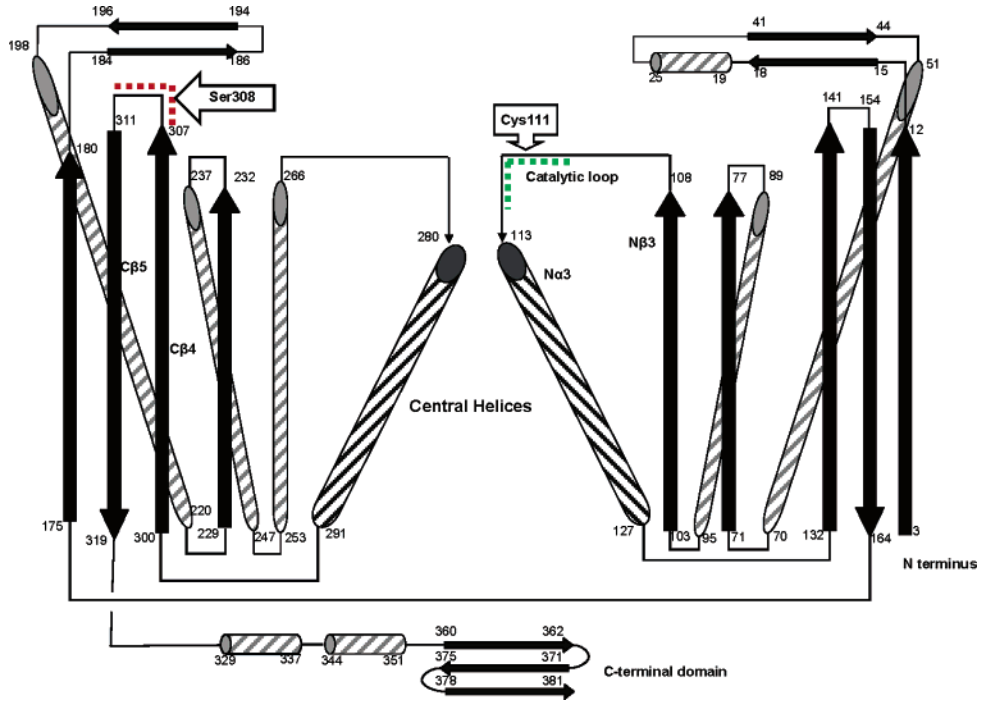

FIGURE 2: Secondary structure topology of the HMG-CoA synthase monomer. The structure of HMG-CoA synthase closely resembles the classic thiolase fold with a duplication of a β-α-β-α-β-α-β-β motif around a 2-fold axis, generating N- and C-terminal subdomains (*19*). The active site loop, denoted in green, connects Nβ3 and Nα3 and contains the cysteine that forms the covalent ligand−enzyme complex characteristic of this family. The residues that conduct the chemistry or ligand selection particular to a member of the thiolase family are located on extended loops between the other secondary structural elements (*37*). The 307−311 loop, highlighted in red and discussed extensively in the text, is located in the C-terminal subdomain between Cβ4 and Cβ5.

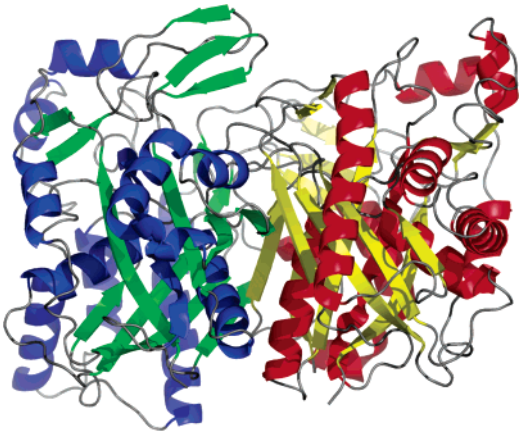

FIGURE 3: Structure of the HMG-CoA synthase dimer with one monomer in red and yellow and the other in blue and green.

pET28b-6H plasmid (*11*) using the QuikChange site-directed mutagenesis kit with primers containing the desired mutation (base changes underlined): 5′-GCTGTTGCTCCGTAACAACCTTCCTTGATTTCGAAAGAGCG-3′ and 5′-CGCTCTTTCGAAATCAAGGAAGGTTGTTACGGAGCAACAGC-3′. Modifications to the procedures of the kit included increasing the annealing temperature to 63 °C and adding 4% dimethyl sulfoxide to the PCR reaction.

Expression and Purification of the Mutant Gene Product. *E. coli* BL21(DE3) pLysS cells transformed with *mvaS*-pET28-6H-Ala110Gly were grown at 25 °C, with shaking, on Luria−Bertani broth (*26*) containing 10 μg of kanamycin/mL and 0.5 mM IPTG. Cells were harvested by centrifugation, washed with 0.9% saline, suspended in 10 mL of 10 mM imidazole in buffer A (300 mM NaCl, 1 mM phenylmethanesulfonyl fluoride, 1 mM dithiothreitol, 20 mM HEPES, pH 8.0), and lysed by sonication. After centrifugation at 30000 rpm for 1 h at 4 °C in a Beckman Optima LE-80K ultracentrifuge, the pellet was discarded, and the supernatant containing mutant protein was loaded onto a 2 mL Talon affinity column and washed with 5 mL of buffer A containing 10 mM imidazole. The mutant protein was eluted with successive 5 mL volumes of buffer A containing 50 mM imidazole in the first volume and 100 mM imidazole in the second. Three milliliter fractions were collected and tested for protein of the correct size by SDS−PAGE. Sigma P8849 cocktail of protease inhibitors was added to fractions containing significant protein to a final concentration of 1% (v/v). The protein concentration of the Ala110Gly mutant protein was determined by the Bradford method (*27*).

HMG-CoA Synthase Activity. HMG-CoA synthase activity was determined using a Hewlett-Packard model 8453 diode array spectrophotometer to monitor the change in absorbance at 302 nm due to the acetyl-CoA-dependent disappearance of the enol form of acetoacetyl-CoA. One enzyme unit (eu) represents the disappearance in 1 min of 1 μmol of acetoacetyl-CoA.

Acetyl-CoA Hydrolase Activity. Acetyl-CoA hydrolase activity was determined by measuring the release of coenzyme A with DTNB [5,5′-dithiobis(2-nitrobenzoic acid)]. The assay employed a Hewlett-Packard model 8453 diode array spectrophotometer with the cell compartment maintained at 37 °C to monitor the change in absorbance at 412 nm that accompanies the reaction of CoA with DTNB (*8*). One eu represents the release in 1 min of 1 μmol of CoA.

Structure Determination. The mutant protein from the above purification scheme was dialyzed against a solution of 300 mM NaCl, 100 mM ammonium sulfate, 5 mM dithiothreitol, and 10 mM HEPES, pH 7.0. It was then

Table 1: Data Collection and Refinement Statistics[a]

data set	A110G mutant
location	APS 14ID-B
energy (keV)	10.000
space group	*I*222
cell dimensions: *a*, *b*, *c* (Å)	105.3, 109.7, 141.9
resolution (Å)	50.0−2.2 (2.28−2.20)
observations	309784
rejections	245 (0.1%)
unique reflections	41829
completeness	99.9 (100.0)
redundancy	7.4 (7.2)
$I/\sigma I$	26.4 (6.4)
R_{merge} (%)	7.1 (26.5)
refinement	
total atoms	6125
protein atoms	5936
waters	258
R_{work}/R_{free} (%)	0.192/0.226
Ramachandran	
core	91.2
allowed	8.5

[a] $R_{merge} = \sum_{hkl}\sum|I - \langle I\rangle|/\sum(I)$, where I is the intensity, $R = \sum|F_o| - |F_c|/\sum|F_o|$, and R_{free} is a control monitoring 1607 reflections left out of the refinement. Data from the last resolution bin are in parentheses.

concentrated to 10 mg/mL with a Centricon spin filter (Millipore) and crystallized in a sitting drop vapor diffusion tray from 2.2 M ammonium sulfate and a buffer of 80 mM HEPES and 20 mM MES at pH 6.2. The crystals grew as bundles of rods, one of which was broken off for the diffraction experiment. The crystal was cryoprotected with 15% glycerol introduced by transferring it in a loop sequentially though a series of drops containing the crystallization reservoir solution with 5%, 10%, and finally 15% glycerol. It was then flash frozen in a 100 K stream of gaseous nitrogen. Diffraction data were collected at the BioCARS beamline (14-ID-B) of the Advanced Photon Source, Argonne National Laboratory. These data were then processed using HKL2000 (*28*) from 50 to 2.2 Å with the reduction and integration statistics shown in Table 1.

Phasing of the data was accomplished by molecular replacement in CNS (*29*) using the previously determined native structure (PDB code 1X9E) as a search model. Immediately following data reduction and integration (*28*) 5% of the reflections were designated with a free-*R* flag and excluded from the refinement process, thus serving as a control against overzealous refinement protocols and the resulting model bias (*30*). After simulated annealing (*31*) the structure was refined using cycles of Powell minimization and *B* factor refinement in CNS alternating with manual side chain adjustment and water additions using O (*32*).

RESULTS

Expression and Purification of the Mutant Enzyme. HMGS Ala110Gly mutant protein was expressed in BL21(DE3) pLysS cells and purified through a modification of the procedure developed for the wild-type synthase (*11*). The mutant enzyme required room temperature and 5 mM IPTG for expression. In addition, a Talon affinity column, which employs Co^{2+} rather than Ni^{2+}, was used. This enzyme preparation scheme yielded approximately 10 mg of protein/L of culture at greater than 95% purity as determined by SDS−PAGE.

Overall Kinetic Parameters. V_{max} for the formation of HMG-CoA from acetyl-CoA and acetoacetyl-CoA was 1440 eu/mg, a rate 140-fold higher than the 10 eu/mg for the wild-type enzyme (*11*). The K_m for acetyl-CoA was 590 μM. The catalytic efficiency, $k_{cat}/K_m^{acetyl-CoA}$, thus had increased 86-fold. Since acetoacetyl-CoA is a competitive inhibitor of the first step of the overall reaction, only a K_m^{app} can be determined, which for the mutant enzyme is 18 μM. Both K_m values are similar to those of the wild-type enzyme (Table 2).

Hydrolysis of Acetyl-CoA. The hydrolysis of acetyl-CoA partially models the first and third steps of the overall reaction, acyl-enzyme formation and enzyme-HMG-CoA hydrolysis, respectively. The hydrolysis of the acetylated enzyme competes with the formation of HMG-CoA but is thought to proceed at only 1% of the overall rate in the native enzyme (*14*). Hydrolysis of the acetyl-CoA was followed by the reaction of the released CoASH with DTNB. This hydrolysis has increased only 37-fold in the mutant enzyme as compared to the 100-fold increase for the overall reaction. The K_m for acetyl-CoA is slightly lower than that for wild type at 1.06 μM. The catalytic efficiency for this reaction has thus increased over 300-fold (Table 2).

Structure. The structure of mutant Ala110Gly HMGS was determined to 2.2 Å resolution (see Materials and Methods) with good statistics (Table 1). Comparison of the mutant protein structure to that of the native enzyme (PDB code 1X9E) demonstrates that the folds of these proteins are virtually identical, with a global rmsd of 0.2 Å over 766 Cα atoms. A visual comparison of the Cα tracings shows that the main chain differences between the two structures are concentrated in two regions. The first is a loop distant from the active site, residues 30, 31, and 32 in the A monomer, that demonstrates a maximal displacement of 1.60 Å. The second is a loop containing residues 307−310 in both monomers (designated by red in Figure 2) that is proximal to the mutation site and the catalytic turn and shows a maximal displacement of 1.15 Å. Aside from this loop shift, the only striking change in the active site is the rotation of the hydroxyl group of serine 308 120° relative to the native side chain. This moves the hydroxyl of Ser308 away from an interaction with Asp184 to now point toward the mutation site (Figure 4). This orientation of Ser308 is a configuration not seen in any of the uninhibited active sites of the HMGS structures published to date (PDB codes 1TXT, 1TVZ, 1XPK, 1XPL, 1XPM, 1X9E) though it was noted as a partial occupancy orientation in the structure of HMGS with acetoacetate bound to the catalytic cysteine (PDB code 1YSL) (*17*). The more common orientation of this hydroxyl side chain is illustrated in Figure 4 by representative native structures of HMGS (PDB codes 1TVZ and 1X9E) and a structure containing a mixture of ligands (PDB code 1XPM).

The mutated active site loop appears to be identical to the native structure except for the missing methyl group of the residue in the $i + 1$ position of the II′ turn (residue 110). The ϕ and ψ values for the glycine are the same as for the alanine in the native structure (+52° and −120°, respectively), and the residues of this mutant loop, including the catalytic cysteine, superimpose on those of the native structure. The remainder of the known catalytically important active site residues, His233 (*33*), Glu79 (*15*), Asp184 (*34*), and Phe185 (*35*), are also unchanged.

Table 2: Kinetic Parameters for Wild-Type and Mutant Ala110Gly *E. faecalis* HMG-CoA Synthase

	overall reaction				hydrolysis of acetyl-CoA		
enzyme	V_{max} (eu/mg)	K_m^{AcCoA} (μM)	$K_m^{AcAcCoA}$ (μM)	k_{cat}/K_m^{AcCoA} ($\mu M^{-1} s^{-1}$)	V_{max} (eu/mg)	K_m^{AcCoA} (μM)	k_{cat}/K_m ($\mu M^{-1} s^{-1}$)
WT[a]	10	350	10	0.02	0.02	8.5	0.00016
A110G	1440	590	18	1.72	0.76	1.06	0.050

[a] Values from wild type as reported in Sutherlin et al. (*11*).

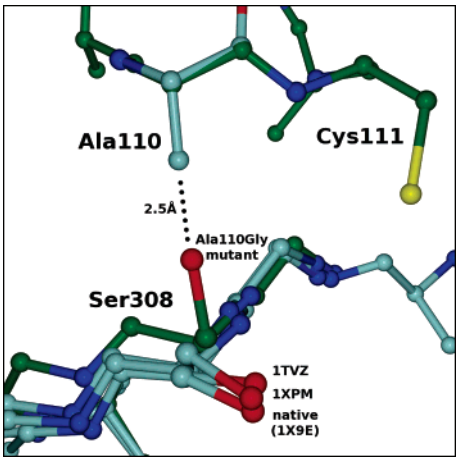

FIGURE 4: Orientation of serine 308 with respect to the active site loop from several published structures of HMG-CoA synthase. The carbons for the Ala110Gly mutant structure are colored green, while the carbons for the native structures are colored blue-gray. The active site loop containing the cysteine that will be acetylated (Cys111) and the site of the Ala110Gly mutation (Ala110) lie across the top of the figure. The configuration of this loop is virtually identical in the mutant and native structures, and this is reflected in the overlapping coloration of the carbons. The 307−311 region that shows the most displacement in the mutant structure compared to the native lies across the bottom. Shown in detail are the orientations of the side chains of serine 308 (or the structurally equivalent serine) for the native structure from *E. faecalis* (labeled native; PDB code 1X9E) (*17*), the mutant, Ala110Gly presented here, the native *S. aureus* (PDB code 1TVZ) (*18*), and the *S. aureus* structure containing bound ligands (PDB code 1XPM) (*16*). The illustrated distance between the mutant serine 308 hydroxyl and the Cβ of the native alanine 110 demonstrates the steric clash that would take place for this configuration in the native enzyme. The alignments were created in O using lsq-exp to match the active site loop residues of the various models (typically to less that 0.01 Å rmsd over residues 109−113) and then moving (lsq-mol) the entire molecule to that orientation. This method allowed observation of even small changes in the distance and orientation of the active site residues relative to Cys111 and Ala/Gly110. The residues shown were edited to remove other side chains and carbonyl groups for clarity of presentation.

DISCUSSION

HMG-CoA synthase plays a key role in ketogenesis in mammalian mitochondria and in isoprenoid formation in the eukaryotic cytosol and in Gram-positive bacteria. As there is only 12% sequence identity among these three types of HMGS, the residues conserved between these isoforms are likely to be important for the function or stability of the enzymes. The differences among these enzymes may be exploited for selective drug design with the unique properties of the cytosolic form being a target for cholesterol-lowering drugs and those of the bacterial enzyme providing clues to the design of new antimicrobial agents.

All HMG-CoA synthases and most members of the extended family of thiolase-fold enzymes have an alanine N-terminal to the catalytic cysteine. The II′ β turn catalytic loop that is characteristic of the thiolase fold forces this alanine to adopt an unusual ϕ angle of +52°. One normally finds a glycine in this position on a II′ β turn, as any side chain larger than a hydrogen will clash with the preceding carbonyl oxygen. We therefore mutated the alanine to a glycine using site-directed mutagenesis, predicting that this change would stabilize the active site loop and so perhaps affect the activity of the enzyme.

Previous studies of the kinetics of HMGS have suggested that the acetylation reaction is the slow step, the condensation of acetoacetyl-CoA with the acetylated-enzyme to be approximately 2-fold faster, and the final hydrolysis of the enzyme-HMG-CoA product complex much faster (*13*, *14*). The Ala110Gly mutation of *E. faecalis* HMGS caused the V_{max} of the overall reaction to increase from 10.0 to 1440 eu/mg, with an 86-fold increase in k_{cat}/K_m. The magnitude of the overall increases in V_{max} and catalytic efficiency suggests that both slow steps, acetyl-enzyme formation and condensation, must be accelerated in the mutant enzyme. There was also an increase in the rate of hydrolysis of acetyl-CoA with an increase in k_{cat}/K_m of over 300-fold. The large increase in catalytic efficiency of the acetyl-CoA hydrolysis half-reaction suggests that the mutation increases the rate of both formation and hydrolysis of the acetyl-enzyme thioester. Thus the mutation of alanine 110 to glycine appears to have affected all three steps of the synthase reaction.

In order to examine the structural basis of this acceleration, we solved the X-ray crystallographic structure of the mutant enzyme and found the overall fold to be very similar to that of the native protein. A close comparison of the two structures shows that the mutation of alanine to glycine causes virtually no change in the configuration of the active site loop, with the glycine adopting the same ϕ and ψ angles of the alanine it replaced. Other residues known to be important in catalysis, such as Glu79 (*15*), Phe185 (*35*), and His233 (*33*), are equally unaffected.

The most striking changes take place in the loop across from the catalytic cysteine comprising residues Gly307 to Ala310. In this region the Cα atoms are shifted toward the mutant Gly110 residue with a maximum displacement of about 1.15 Å for the Cα of Gly309. This is a considerable shift when seen against a background average rmsd of 0.2 Å over the 766 atoms in the dimer. The other significant change is seen in the Ser308 side chain that rotates approximately 120° from its native position to point toward the active site loop (Figure 4). In reviewing all of the active sites represented in the eight available HMGS structures (19 total), this positioning of Ser308 is not present in any of the native structures, nor in the structures containing various combinations of ligands. It is only seen in the mutant structure presented here and as a partially occupied position in the HMGS structure from *E. faecalis* that is covalently inhibited by an acetoacetyl group bound to the catalytic cysteine (PDB code 1YSL) (*17*). This suggests that the

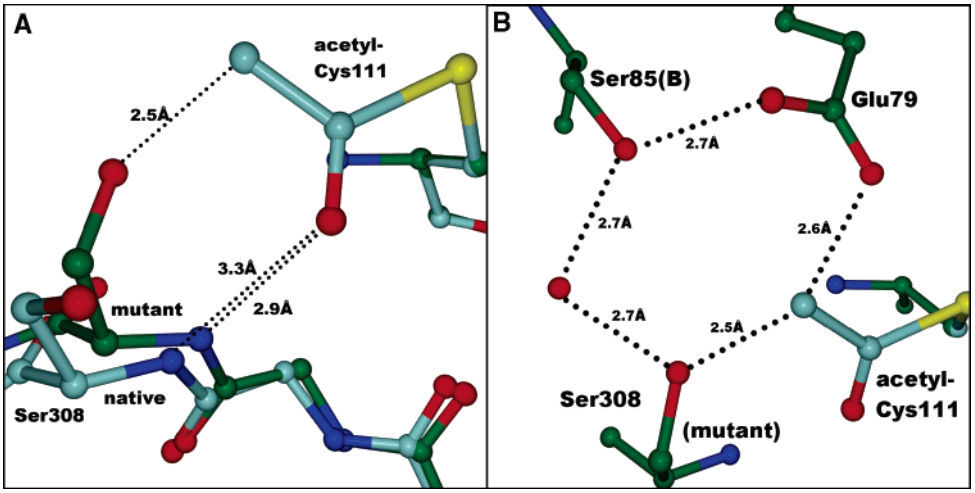

FIGURE 5: Interactions between a modeled acetyl-enzyme intermediate and the conformational adaptations of the Ala110Gly mutation in HMGS. Panel A: Loop 307−311 shifts, bringing the amide nitrogen of Ser308 closer to the carbonyl oxygen of the acetyl-enzyme thioester. Panel B: The hydrogen-bonding pattern around the methyl group of the acyl-enzyme intermediate acts to stabilize the formation of the carbanion. This then serves as a nucleophile that attacks the second substrate, acetoacetyl-CoA, during the condensation reaction. The rotation of Ser308 induced by the Ala110Gly mutation brings the hydroxyl of Ser308 closer to the carbanion, further increasing the stabilization of this reaction intermediate. Serine 85 is from the adjacent monomer (B) of the dimeric enzyme. The position of the acetylcysteine was modeled using the residue from the *S. aureus* structure of HMGS (PDB code 1XPM) (*16*), moving it to exactly match the N, Cα, C*β*, C, and O main chain atoms of the equivalent residue in the Ala110Gly mutant. The color scheme for the backbone atoms and the positioning of the native (PDB code 1X9E) (*17*) serine 308 vs the Ala110Gly mutant in panel A was the same as that described in Figure 4.

orientation of Ser308 seen in the Ala110Gly mutant is possible in the native protein during the course of the reaction, but perhaps only when a larger ligand than acetate is bound to the catalytic cysteine.

The question then is how do these structural changes account for the remarkable increase in the rate of reaction and catalytic efficiency of the Gly110Ala mutant enzyme? The removal of the C*β* atom from residue 110 by mutation from alanine to glycine clears a space that allows both the rotation of the serine hydroxyl and the movement of the Ser308 loop closer to Cys111, as illustrated by the close contact of the mutant-oriented Ser308 and the C*β* of the native Ala110 in Figure 4. To study the implications of these motions, we made a model of the acyl-enzyme complex using the acylcysteine residue from the *S. aureus* HMGS structure, 1XPM (monomer D), and superimposing the common atoms on our catalytic cysteine. From this construct it became clear that the movement of the Ser308 loop brought the amide nitrogen of Ser308 closer to the carbonyl of the acyl group by about 0.4 Å (Figure 5, panel A). This shorter hydrogen bond would lead to tighter binding of the acyl group, which is reflected in the decreased K_m of the hydrolysis half-reaction. The movement of this loop would also have a direct stabilizing effect on the catalytic intermediate. The interaction between this amide and the oxygen has previously been identified as an "oxyanion hole" (*18*), defined here as a main chain nitrogen that catalyzes a nucleophilic attack on a carbonyl carbon by stabilizing the negative charge on the carbonyl oxygen in the tetrahedral intermediate. As the loop moves toward the acetyl group, the hydrogen bond from the amide nitrogen to the carbonyl oxygen decreases from 3.3 to 2.9 Å (Figure 5, panel A). Closer interaction between these two atoms provides a more potent stabilizing force which would lower the energy barrier for the reaction and lead to a faster rate. This configuration would stabilize the reaction intermediate in both the formation of the acyl-enzyme intermediate (where the sulfur of the cysteine is the nucleophile) and the hydrolysis reaction (where water is the nucleophile), accounting for the remarkable rate increase seen for the acyl-CoA hydrolysis half-reaction in the Ala110Gly mutant enzyme.

The repositioning of the hydroxyl of Ser308 in the Ala110Gly mutant plays a central role in the increased overall catalytic rate. From the same acyl-enzyme construct of the mutant protein the serine side chain is seen to be within hydrogen-bonding distance of the methyl group of the acetyl ligand (Figure 5, panel B). This unusual proximity to the methyl group is allowed because the acetylcysteine methyl is converted to a carbanion by an interaction with Glu79 (*16*) to serve as a nucleophile in the condensation reaction with the second substrate, acetoacetyl-CoA. Figure 5, panel B, illustrates that the serine hydroxyl of the mutant is in a position to help to stabilize the negative charge on the methyl carbon by both a hydrogen-bonding interaction and positioning the carbanion to optimize its interaction with Glu79. Both kinds of interaction, enthalpic and entropic, contribute to lowering the activation energy of the condensation step. These effects, in combination with the increased rate of acetyl-enzyme formation, the rate-determining step for the overall reaction, account for the remarkably accelerated velocity of the Ala110Gly mutant enzyme.

This interpretation of the enzymatic consequences of the Ala110Gly mutation is reinforced by published research on the HMG-CoA synthase from *Brassica juncea* (*36*). In this study Nagegowada and co-workers cloned and expressed a plant HMGS and studied the enzymatic effects of a series of mutations. The one of interest in the context of this discussion is the mutation to alanine of Ser359, which by sequence alignment is equivalent to Ser308 in HMGS from *E. faecalis*. Their kinetic studies show this mutation increases the V_{max} and k_{cat} of the overall reaction 8.5-fold and decreases the $t_{1/2}$ of the acetyl-CoA hydrolysis from 11.1 min for the wild type to 4.7 min for the mutant enzyme. These results are consistent with the involvement of the conserved serine

in our proposed mechanism. Mutating this serine to an alanine shortens the side chain by removing the terminal hydroxyl. The reduction in size of this side chain would allow the backbone in this region to move closer to the catalytic loop just as the removal of the Cβ carbon from Ala110 does in the *E. faecalis* mutant (Figures 4 and 5). Thus the amide nitrogen of the mutated serine could be closer to the carbonyl oxygen of the acetate group just as it is in Ala110Gly HMGS, speeding up both the overall reaction and the acetyl-CoA hydrolysis. However, because the plant mutation removed the hydroxyl from the Ser308 equivalent, this active site residue would no longer be able to provide the stabilization of the carbanion intermediate in the condensation step discussed above. The kinetic consequence of this would be that the rate of the condensation reaction in the plant enzyme would not be increased, and this step would now be the slow step in the reaction sequence. Thus, the overall V_{max} of the plant mutant enzyme does not increase as sharply as our Ala110Gly mutation that is able to accelerate both of the slow steps of the reaction pathway.

Finally, one needs to ask the question as to why nature would select for an enzyme with less than optimal catalytic efficiency. The answer may be in the need to balance the flux of high-energy metabolic intermediates. In animals, a more efficient mitochondrial HMG-CoA synthase would have the effect of siphoning off acetyl-CoA from the TCA cycle to either create a futile cycle of acetyl-CoA hydrolysis or inappropriately producing ketone bodies even in the fed state. In bacteria the same balance between the parsimonious use of acetyl-CoA for catabolism or anabolism should hold true, and the "structural governor" incorporated into the HMGS structure may prove to be a key factor in maintaining metabolic balance.

In the broader family of enzymes that share the thiolase fold, the $i + 1$ position of the II′ β, catalytic turn continues to be conserved as a non-glycine residue with a strained ϕ angle. As presented here, in HMG-CoA synthase it appears that one role of this side chain is to exclude the hydroxyl of serine 308 from interacting with the acyl-enzyme thiolase bond. This limits the V_{max} of the overall reaction and the premature hydrolysis of the initial acyl-enzyme intermediate. However, most of the wider family of thiolase structure enzymes appear to lack the structural equivalent of serine 308. What then is the purpose of the Cβ carbon in the $i + 1$ position in these enzymes? The enzymes of the thiolase-fold family catalyze diverse reactions but have a common acyl-enzyme intermediate with the acyl group bound to the catalytic cysteine by a thioester bond (*37*). A bulky residue in the $i + 1$ position would be in position to block solvent access to that thioester bond. Mutation of that residue to the much more commonly found glycine might, as in the case of the Ala110Gly mutation of HMG-CoA synthase, lead to a futile cycle of rapid, premature hydrolysis of the acyl-enzyme intermediate and, so, loss of valuable energetic metabolites to the organism. A direction for future research might be to pursue this hypothesis by mutating the $i + 1$ residues of other members of the thiolase family and use kinetics and structure to demonstrate their role in the catalytic process.

ACKNOWLEDGMENT

The authors gratefully acknowledge the able and enthusiastic assistance provided by the staff of the Advanced Photon Source, Argonne National Laboratory, beamline 14ID. Without the capabilities of this marvelous institution this project would not have happened.

REFERENCES

1. Alberts, B., Bray, D., Lewis, J., Raff, M., Roberts, K., and Watson, J. D. (1989) *Molecular Biology of the Cell*, Garland Publishing, New York.
2. Lange, B. M., Rujan, T., Martin, W., and Croteau, R. (2000) Isoprenoid Biosynthesis: The Evolution of Two Ancient and Distinct Pathways Across Genomes, *Proc. Natl. Acad. Sci. U.S.A. 97*, 13172−13177.
3. Reusch, V. M., Jr. (1984) Lipopolymers, Isoprenoids, and the Assembly of the Gram-Positive Cell Wall, *Crit. Rev. Microbiol. 11*, 129−155.
4. Meganathan, R. (1996) Biosynthesis of the Isoprenoid Quinines Menaquinone (Vitamin K_2) and Ubiquinone (Coenzyme Q), in *Escherichia coli and Salmonella: Cellular and Molecular Biology* (Neidhardt, F. C., Curtiss, R., III, Ingraham, J. L., Lin, E. C. C., Low, K. B., Magasanik, B., Reznikoff, W. S., Riley, M., Schaechter, M., and Umbarger, H. E., Eds.) 2nd ed., Vol. 1, pp 642−656, American Society for Microbiology, Washington, DC.
5. Johnson, E. A., and Schroeder, W. A. (1996) Microbial carotenoids, *Adv. Biochem. Eng. Biotechnol. 53*, 119−178.
6. Wilding, E. I., Kim, D. Y., Bryant, A. P., Gwynn, M. N., Lunsford, R. D., McDevitt, D., Myers, J. E., Jr., Rosenberg, M., Sylvester, D., Stauffacher, C. V., and Rodwell, V. W. (2000) Essentiality, Expression, and Characterization of the Class II 3-Hydroxy-3-Methylglutaryl Coenzyme A Reductase of *Staphylococcus aureus*, *J. Bacteriol. 182*, 5147−5152.
7. Wilding, E. I., Brown, J. R., Bryant, A. P., Chalker, A. F., Holmes, D. J., Ingraham, K. A., Iordanescu, S., So, C. Y., Rosenberg, M., and Gwynn, M. N. (2000) Identification, Evolution, and Essentiality of the Mevalonate Pathway for Isopentenyl Diphosphate Biosynthesis in Gram-Positive Cocci, *J. Bacteriol. 182*, 4319−4327.
8. Istvan, E. S. (2001) Bacterial and Mammalian HMG-CoA Reductases: Related Enzymes with Distinct Architectures, *Curr. Opin. Struct. Biol. 11*, 746−751.
9. Bochar, D. A., Stauffacher, C. V., and Rodwell, V. W. (1999) Sequence Comparisons Reveal Two Classes of 3-Hydroxy-3-Methylglutaryl Coenzyme A Reductase, *Mol. Genet. Metab. 66*, 122−127.
10. Hedl, M., Tabernero, L., Stauffacher, C. V., and Rodwell, V. W. (2004) Class II 3-Hydroxy-3-Methylglutaryl Coenzyme A Reductases, *J. Bacteriol. 186*, 1927−1932.
11. Sutherlin, A., Hedl, M., Sanchez-Neri, B., Burgner, J. W., Stauffacher, C. V., and Rodwell, V. W. (2002) *Enterococcus faecalis* 3-Hydroxy-3-Methylglutaryl Coenzyme A Synthase, an Enzyme of Isopentenyl Diphosphate Biosynthesis, *J. Bacteriol. 184*, 4065−4070.
12. Middleton, B. (1972) Kinetic Mechanism of 3-Hydroxy-3-Methylglutaryl-Coenzyme-A Synthase from Bakers' Yeast, *Biochem. J. 126*, 35−47.
13. Miziorko, H. M., and Lane, M. D. (1977) 3-Hydroxy-3-Methylgutaryl-CoA Synthase. Participation of Acetyl-S-Enzyme and Enzyme-S-Hydroxymethylgutaryl-SCoA Intermediates in the Reaction, *J. Biol. Chem. 252*, 1414−1420.
14. Miziorko, H. M., Clinkenbeard, K. D., Reed, W. D., and Lane, M. D. (1975) 3-Hydroxy-3-Methylglutaryl Coenzyme A Synthase. Evidence for an Acetyl-S-Enzyme Intermediate and Identification of a Cysteinyl Sulfhydryl as the Site of Acetylation, *J. Biol. Chem. 250*, 5768−5773.
15. Chun, K. Y., Vinarov, D. A., Zajicek, J., and Miziorko, H. M. (2000) 3-Hydroxy-3-Methylglutaryl-CoA Synthase−A Role for Glutamate 95 in General Acid/Base Catalysis of C-C Bond Formation, *J. Biol. Chem. 275*, 17946−17953.
16. Theisen, M. J., Misra, I., Saadat, D., Campobasso, N., Miziorko, H. M., and Harrison, D. H. T. (2004) 3-Hydroxy-3-Methylglutaryl-CoA Synthase Intermediate Complex Observed in "Real-Time", *Proc. Natl. Acad. Sci. U.S.A. 101*, 16442−16447.

17. Steussy, C. N., Vartia, A. A., Burgner, J. W., II, Sutherlin, A., Rodwell, V. W., and Stauffacher, C. V. (2005) X-ray Crystal Structures of HMG-CoA Synthase from *Enterococcus faecalis* and a Complex with its Second Substrate/Inhibitor Acetoacetyl-CoA, *Biochemistry 44*, 14256−14267.
18. Campobasso, N., Patel, M., Wilding, I. E., Kallender, H., Rosenberg, M., and Gwynn, M. N. (2004) *Staphylococcus aureus* 3-Hydroxy-3-Methylglutaryl-CoA Synthase−Crystal Structure and Mechanism, *J. Biol. Chem. 279*, 44883−44888.
19. Huang, W., Jia, J., Edwards, P., Dehesh, K., Schneider, G., and Lindqvist, Y. (1998) Crystal Structure of Beta-Ketoacyl-Acyl Carrier Protein Synthase II from *E. coli* Reveals the Molecular Architecture of Condensing Enzymes, *EMBO J. 17*, 1183−1191.
20. Kursula, P., Sikkila, H., Fukao, T., Kondo, N., and Wierenga, R. K. (2005) High Resolution Crystal Structures of Human Cytosolic Thiolase (CT): A Comparison of the Active Sites of Human CT, Bacterial Thiolase, and Bacterial KAS I, *J. Mol. Biol. 347*, 189−201.
21. Ferrer, J. L., Jez, J. M., Bowman, M. E., Dixon, R. A., and Noel, J. P. (1999) Structure of Chalcone Synthase and the Molecular Basis of Plant Polyketide Biosynthesis, *Nat. Struct. Biol. 6*, 775−784.
22. Olsen, J. G., Kadziola, A., Wettstein-Knowles, P., Siggaard-Andersen, M., Lindquist, Y., and Larsen, S. (1999) The X-Ray Crystal Structure of Beta-Ketoacyl [Acyl Carrier Protein] Synthase I, *FEBS Lett. 460*, 46−52.
23. Qiu, X., Janson, C. A., Konstantinidis, A. K., Nwagwu, S., Silverman, C., Smith, W. W., Khandekar, S., Lonsdale, J., and Abdel-Meguid, S. S. (1999) Crystal Structure of Beta-Ketoacyl-Acyl Carrier Protein Synthase III, *J. Biol. Chem. 274*, 36465−36471.
24. Stites, W. E., Meeker, A. K., and Shortle, D. (1994) Evidence for Strained Interactions between Side-Chains and the Polypeptide Backbone, *J. Mol. Biol. 235*, 27−32.
25. Hutchinson, E. G., and Thornton, J. M. (1994) A Revised Set of Potentials for Beta-Turn Formation in Proteins, *Protein Sci. 3*, 2207−2216.
26. Sambrook, J., Fritsch, E. F., and Maniatis, T. (1987) *Molecular Cloning: A Laboratory Manual*, 2nd ed., Cold Spring Harbor Laboratory Press, Cold Spring Harbor, NY.
27. Bradford, M. M. (1976) A Rapid and Sensitive Method for the Quantitation of Microgram Quantities of Protein Utilizing the Principle of Protein-Dye Binding, *Anal. Biochem. 72*, 248−254.
28. Otwinowski, Z., and Minor, W. (1997) Processing of X-Ray Diffraction Data Collected in Oscillation Mode, in *Macromolecular Crystallography* (Carter,C. W., and Sweet, R. M., Eds.) pp 307−326, Academic Press, New York.
29. Brunger, A. T., Adams, P. D., Clore, G. M., Delano, W. L., Gros, P., Grosse-Kunstleve, R. W., Jiang, J. S., Kuszewski, J., Nilges, M., Pannu, N. S., Read, R. J., Rice, L. M., Simonson, T., and Warren, G. L. (1998) Crystallography & NMR System: A New Software Suite for Macromolecular Structure Determination, *Acta Crystallogr., Sect. D: Biol. Crystallogr. 54* (Part 5), 905−921.
30. Brunger, A. T. (1992) Free R Value: A Novel Statistical Quantity for Assessing the Accuracy of Crystal Structures, *Nature 355*, 472−475.
31. Adams, P. D., Pannu, N. S., Read, R. J., and Brunger, A. T. (1997) Cross-Validated Maximum Likelihood Enhances Crystallographic Simulated Annealing Refinement, *Proc. Natl. Acad. Sci. U.S.A. 94*, 5018−5023.
32. Kleywegt, G., and Jones, A. (1997) Model Building and Refinement Practice, in *Macromolecular Crystallography* (Carter, C. W., and Sweet, R. M., Eds.) pp 208−229, Academic Press, New York.
33. Misra, I., and Miziorko, H. M. (1996) Evidence for the Interaction of Avian 3-Hydroxy-3-Methylglutaryl-CoA Synthase Histidine 264 with Acetoacetyl-CoA, *Biochemistry 35*, 9610−9616.
34. Chun, K. Y., Vinarov, D. A., and Miziorko, H. M. (2000) 3-Hydroxy-3-Methylglutaryl-CoA Synthase: Participation of Invariant Acidic Residues in Formation of the Acetyl-S-Enzyme Reaction Intermediate, *Biochemistry 39*, 14670−14681.
35. Misra, I., Wang, C. Z., and Miziorko, H. M. (2003) The Influence of Conserved Aromatic Residues in 3-Hydroxy-3-Methylglutaryl-CoA Synthase, *J. Biol. Chem. 278*, 26443−26449.
36. Nagegowda, D. A., Bach, T. J., and Chye, M. L. (2004) *Brassica juncea* 3-Hydroxy-3-Methylglutaryl (HMG)-CoA Synthase 1: Expression and Characterization of Recombinant Wild-Type and Mutant Enzymes, *Biochem. J. 383*, 517−527.
37. Haapalainen, A. M., Merilainen, G., and Wierenga, R. K. (2006) The Thiolase Superfamily: Condensing Enzymes with Diverse Reaction Specificities, *Trends Biochem. Sci. 31*, 64−71.

BI061505Q